FUNDAMENTAL CHARACTERISTICS OF HIGH MODULUS CFRP MATERIALS FOR STRENGTHENING OF STEEL-CONCRETE COMPOSITE BEAMS

Mina Dawood, Sami Rizkalla and Emmett Sumner
Constructed Facilities Laboratory
North Carolina State University
2414 Campus Shore Drive
Campus Box 7533
Raleigh, NC, USA, 27695-7533
sami_rizkalla@ncsu.edu

KEYWORDS: CFRP, steel structures, strengthening, flexure, bond,

ABSTRACT
This paper presents the findings of a research program which was conducted to investigate the fundamental behavior of steel-concrete composite beams strengthened with high modulus (HM) carbon fiber reinforced polymer (CFRP) materials. The first part of this paper presents a brief description of the HM CFRP materials and the adhesive selection. The second part of the paper focuses primarily on the flexural behavior of steel-concrete composite beams strengthened with CFRP laminates. The behavior of steel-concrete composite beams strengthened with different configurations of CFRP materials and loaded under monotonic, overloading and fatigue loading conditions is presented. Based on the findings of the experimental program flexural design guidelines are proposed to facilitate the design of the CFRP strengthening for steel bridges and structures. The final section of the paper discusses in detail the bond behavior of the CFRP laminates. The bond behavior is investigated using both double-lap shear coupon tests and large-scale flexural tests. The effectiveness of implementing a reverse taper at the end of the CFRP plates is investigated as a means of enhancing the bond characteristics. The proposed analytical tools and finite element analysis, used to predict the bond behavior of the CFRP bonded joints, are in good correlation with the experimental results. This paper demonstrates that high modulus CFRP materials can be effectively implemented for strengthening and repair of steel bridges and structures.

INTRODUCTION

Recently, considerable research has been conducted on the use of carbon fiber reinforced polymer (CFRP) materials for rehabilitation and strengthening of steel bridges and structures (Mertz & Gillespie, 1996; Sen et al., 2001; Liu et al., 2001, Tavakkolizadeh and Saadatmanesh, 2003; Al-Saidy et al., 2005; Lenwari et al., 2005). The previous research indicates that externally bonded CFRP laminates can be used to increase the ultimate strength of steel girders and to restore the lost capacity and stiffness of damaged or deteriorated girders. However, due to the relatively low modulus of elasticity of conventional CFRP materials as compared to steel, large amounts of strengthening materials are required to achieve a significant increase of the elastic stiffness. The use of high modulus CFRP (HM CFRP) materials has been demonstrated to be a more effective technique to increase the stiffness of steel beams (Rizkalla and Dawood, 2006).

HIGH MODULUS CFRP MATERIALS

High modulus carbon fiber materials are commonly produced as dry fiber tow sheets. The sheets can be impregnated with a saturating resin on-site using a wet lay-up technique and are well suited for application on curved or highly irregular surfaces. For applications requiring a higher degree of strengthening, the carbon fibers can also be pultruded into a precured laminate which can be subsequently bonded to the surface of the structure using a structural adhesive. The typical material properties of the dry fibers and pultruded laminate HM CFRP materials are given in Table 1 .

Table 1: HM carbon fiber material properties

	Fiber Properties (Mitsubishi, 2004)	Laminate Properties
Tensile modulus of elasticity, E	640 GPa	460 GPa
Tensile ultimate strength, f_u	2600 MPa	1540 MPa
Tensile rupture strain, ε_u	0.004	0.0033
Fiber volume fraction, FVF	-	70%

ADHESIVE SELECTION

The first phase of the research program focused on the selection of a suitable adhesive to bond carbon fiber laminates to steel surfaces (Schnerch, 2005). A total of six different adhesives were evaluated using small scale flexural tests. The test specimens consisted of an 813 mm long steel I-beam with a steel plate welded to the compression flange to simulate the presence of a composite concrete deck slab. The beams were strengthened by bonding 36 mm wide x 1.4 mm thick CFRP laminates of varying lengths to the bottom of the tension flange. The beams were subsequently loaded to failure in a four point bending configuration. Of the six adhesives tested, the SP Spabond 345 two part epoxy adhesive was capable of developing the full rupture strength of the 1.4 mm thick HM CFRP strips within a development length of 102 mm. Due to its relatively short development length and its workability and suitability for overhead application, this adhesive was selected for the remaining study of the behavior of the CFRP strengthening system.

FLEXURAL BEHAVIOR

Once a suitable adhesive was identified, the fundamental behavior of steel-concrete composite beams strengthened with CFRP materials was investigated. Three 6400 mm long steel-concrete composite beams were tested to investigate the effectiveness of using different configurations of CFRP laminates to increase the strength and stiffness of typical steel highway bridge girders. The configurations studied included externally bonded high modulus (HM) CFRP laminates, externally bonded intermediate modulus (IM) CFRP laminates and prestressed high modulus CFRP laminates. A detailed description of the study is presented by Schnerch (2005). The load-deflection behavior of the three tested beams is presented in Figure 1(a). The ultimate capacity of the beams was governed by rupture of the CFRP as shown in Figure 1. Failure occurred due to crushing of the concrete in all three cases. A typical beam after failure is shown in Figure 1(b). Installation of both the intermediate modulus and the high modulus CFRP materials effectively increased the elastic stiffness and the ultimate capacity of the strengthened beams. Alternatively, the prestressed CFRP system was designed primarily to increase the stiffness of the beam without increasing the ultimate capacity of the member. This may be advantageous in cases where it is desired to improve the serviceability of a member while maintaining the full ductility of the unstrengthened section.

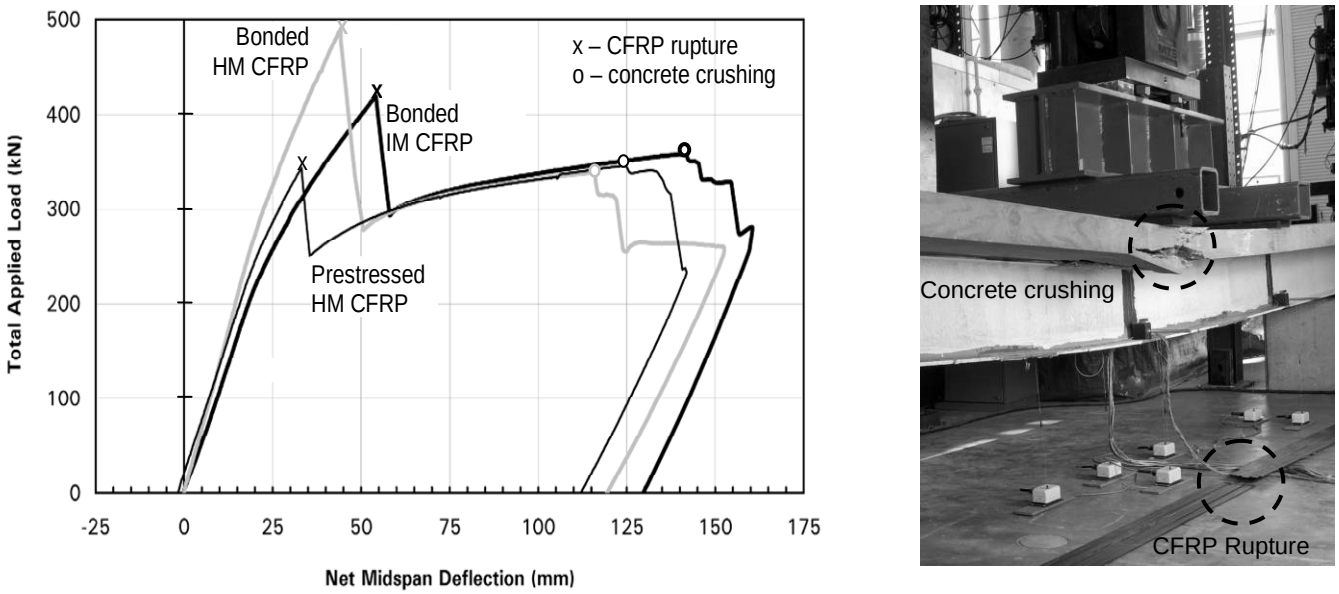

(a) Load-deflection behavior (b) Typical beam failure

Figure 1 Flexural behavior of large-scale beams strengthened with CFRP laminates

FATIGUE LOADING AND OVERLOADING BEHAVIOR

An additional six scaled steel-concrete composite beams were tested to study the behavior of the strengthening system under fatigue loading and overloading conditions as presented in detail in Dawood (2005). The typical test beams were tested in four-point bending with a span of 3050 mm and a 610 mm long constant moment region.

Two of the test beams were strengthened with different reinforcement ratios of high modulus CFRP materials and subjected to several loading and unloading cycles to simulate severe overloading conditions. A third unstrengthened beam was tested as a control beam for comparison purposes. The typical load-deflection behavior of an unstrengthened beam and a strengthened beam are shown in Figure 2(a). In addition to increasing the ultimate capacity and elastic stiffness of the beams, installation of the high modulus CFRP materials also helped to increase the yield load of the beams as shown in the figure. Figure 2(a) also indicates that the presence of the CFRP materials significantly reduced the residual deflection of the strengthened beam due to the simulated overloading conditions as compared to the unstrengthened control beam. This suggests that in the event of overloading conditions, an unstrengthened beam would likely exhibit a significant residual deflection which may necessitate replacement of the member while a similar strengthened beam would remain in excellent serviceable condition.

The remaining three test beams were tested under fatigue loading conditions. Two of the beams were strengthened using the same reinforcement ratio of CFRP materials however, using different bonding techniques to investigate the effect of the bond on the fatigue performance of the system. The third beam remained unstrengthened to serve as a control beam for the fatigue study. All three of the test beams were subjected to three million fatigue loading cycles. The minimum applied load used for the cyclic loading for all three beams was selected to be equivalent to 30 percent of the calculated yield load of the unstrengthened beams to simulate the effect of the sustained dead-load for a typical bridge structure. For the unstrengthened beam, the maximum load in the loading cycle was selected to be equivalent to 60 percent of the calculated yield load to simulate the combined effect of dead-load and live-load. The maximum load for the two strengthened beams was selected to be equivalent to 60 percent of the calculated increased yield load of the strengthened beams. The maximum load simulated an increase of 20 percent of the allowable live-load level in comparison to the unstrengthened

beam. The two strengthened beams were capable of sustaining three million load cycles at the increased simulated live load level without exhibiting any indication of failure. All three beams demonstrated minimal degradation of the elastic stiffness throughout the three million cycle loading course as shown in Figure 2(b). However, the unstrengthened beam exhibited an increase of the mean deflection of approximately 30 percent, which was likely due to the fatigue-creep behavior of the concrete deck, while the strengthened beams exhibited a superior performance as shown in Figure 2(c).

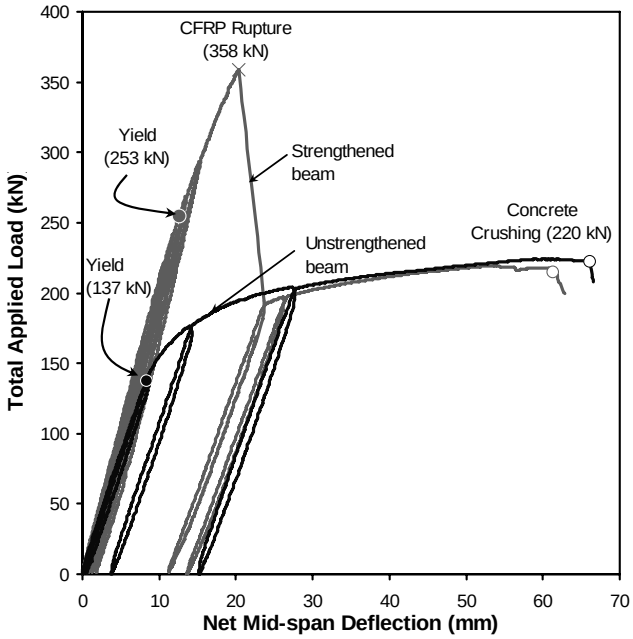

(a) Load-deflection behavior due to simulated overloading

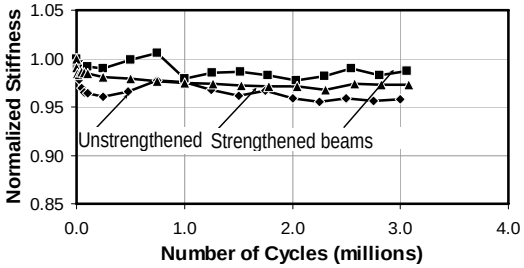

(b) Stiffness degradation due to fatigue

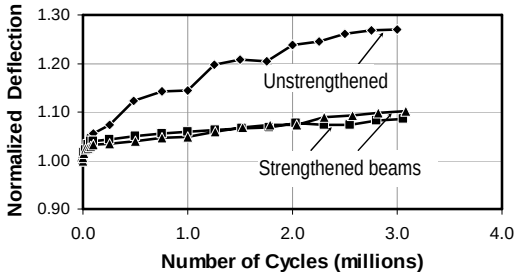

(c) Mean deflection degradation due to fatigue

Figure 2 Overloading and fatigue behavior of strengthened steel-concrete composite beams

FLEXURAL DESIGN GUIDELINES

The design of the CFRP strengthening materials to achieve a specified increase of the allowable live load level for a steel girder is based on a moment-curvature analysis which satisfies equilibrium and compatibility and accounts for the non-linear characteristics of the concrete deck slab and the steel girder. The analysis procedure and a worked example of the proposed design guidelines are presented in detail elsewhere (Schnerch et al., 2006). The increased live load level of the strengthened member should satisfy three conditions as shown in Figure 3 relative to the moment-curvature relationship of a typical strengthened steel-concrete composite beam. To ensure that the beam remains elastic under service loading conditions, the combined effect of the dead load, M_D, and the increased live load, M_L, should not exceed 60 percent of the increased yield load of the strengthened member, $M_{y,S}$. Additionally, to satisfy the strength limit state, the total factored load, after applying the appropriate dead and live load factors, α_D and α_L respectively, should not exceed the ultimate capacity of the strengthened member, $M_{U,S}$, after applying an appropriate strength reduction factor, ϕ. A strength reduction factor of 0.75 is proposed which is consistent with the American Institute of Steel Construction (AISC) requirements for rupture type limit states (2001). To ensure the safety of the structure in the event of a sudden loss of the strengthening system, the total effect of the applied dead load, M_D, and the increased live load, M_L, should not exceed the residual nominal capacity of the unstrengthened beam, $M_{n,US}$.

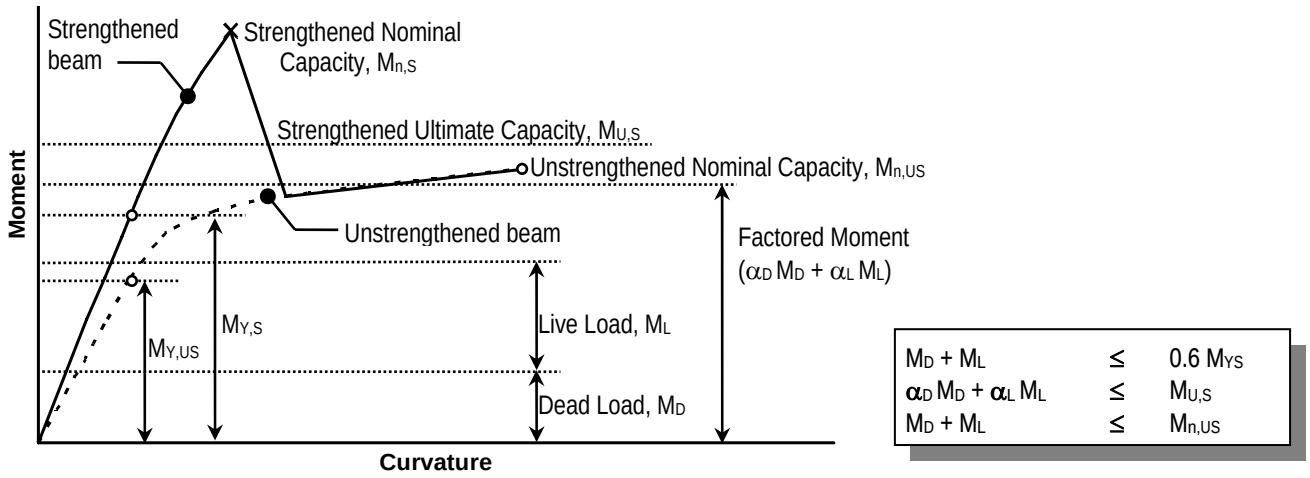

Figure 3 Proposed design criteria for strengthening of steel beams with HM CFRP materials

BOND BEHAVIOR

While the flexural behavior of steel girders strengthened with FRP materials is relatively well understood, the bond behavior is considerably more complex and less well understood. Similarly to reinforced concrete beams, for steel beams reinforced with externally bonded CFRP materials, the bond stresses at the interface between the beam and the strengthening materials, including both shear and peeling components, must be carefully considered to prevent premature debonding failures (Buyukozturk et al., 2003).

Lenwari et al. (2006) proposed a fracture mechanics based approach to calculate the debonding strength of a bonded joint. They indicate that debonding typically occurs due to a stress singularity which forms at the interface between the steel and the adhesive near the end of the strengthening plate. They further indicated that increasing the thickness of the adhesive layer and providing a spew fillet at the end of the bonded joint are effective means of reducing the intensity of the stress singularity and therefore also increasing the capacity of a bonded joint.

A number of other researchers have developed analytical models, which employ a stress-based approach to predict the shear and peeling stress distribution for steel beams strengthened with an adhesively bonded plate (Smith and Teng, 2001; Schnerch, 2005; Stratford and Cadei, 2006). These models predict that the bond stresses are highest near the end of the strengthening plate due to stress concentrations which typically form due to the abrupt termination of the strengthening. Stratford and Cadei (2006) demonstrated analytically that these stress concentrations can be reduced by gradually tapering the end of the strengthening plate. Finite element analysis results further indicate that implementing a reverse taper and a spew fillet near the end of a bonded joint can also effectively reduce the maximum shear and peeling stress concentrations near the end of the joint (Belingardi et al., 2002; Hildebrand, 1994).

Bond stresses are particularly critical at lap-spliced connections between CFRP laminates. These types of joints can facilitate implementation of the CFRP strengthening system to longer span bridges and girders. The behavior of these splices is dramatically affected by the bond behavior and the bond stress distribution between the FRP laminates. There have only been a limited number of studies which investigate the behavior of spliced connections of CFRP laminates under flexural loading. Stallings and Porter tested eight reinforced concrete beams strengthened with various configurations of externally bonded CFRP splice joints (2003). They recommend that in order to prevent debonding of the CFRP splice plate, the maximum strain in the main CFRP plate immediately prior to the splice should not exceed a limiting value. To the authors knowledge there have not been any studies investigating the splice behavior of steel beams reinforced with CFRP laminates.

Experimental Program

An experimental program was conducted in two phases to investigate the bond and splice behavior of CFRP laminates. In the first phase three different configurations of double-lap shear coupons, shown schematically in Figure 4(a) – (c), were tested. The objective of the first phase was to determine the effectiveness of implementing a reverse taper detail at various critical locations throughout the spliced joint. The splice coupons were 35 mm wide and were fabricated from 4 mm thick CFRP laminates with a modulus of elasticity of 460 GPa and an ultimate strain of 0.0033 as reported by the manufacturer. For all three joint configurations, strains were measured at various locations along the splice joint using electrical resistance strain gauges.

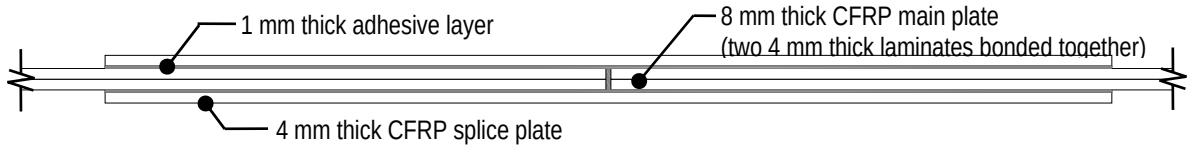

(a) Configuration A (square ends, no fillet)

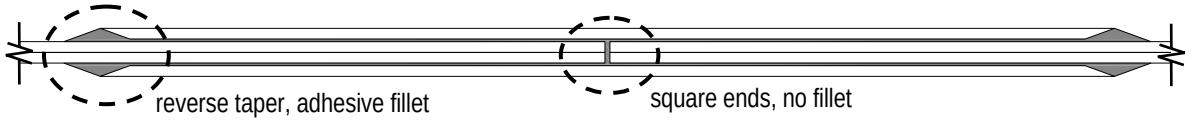

(b) Configuration B

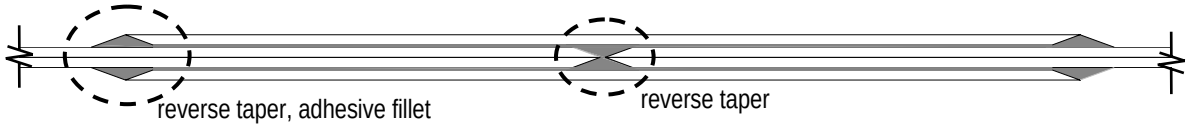

(c) Configuration C

Figure 4 Double-lap shear coupon joint configurations and instrumentation

In the second phase of the experimental program, two steel beams were tested to investigate the behavior of spliced joints under flexural loading conditions. A typical test beam is shown schematically in Figure 5. The beams each consisted of a standard W12x30 steel beam with a C9x15 steel channel welded to the top flange to simulate the presence of a reinforced concrete deck. Each test beam was strengthened by bonding a 100 mm wide by 4 mm thick HM CFRP laminate to the tension flange. The laminate was left discontinuous at the midspan of the beam as shown in Detail A of Figure 5. Continuity of the strengthening system was provided by bonding an 800 mm long CFRP splice plate at the joint location which overlapped 400 mm on either side of the CFRP main plate. All of the plate ends were left square without incorporating a reverse taper to serve as a reference for future tests which will incorporate different joint details. Due to the high level of uncertainty associated with the bond behavior, two such beams were tested to provide repeated test data for a given splice configuration. The strengthened beams were loaded monotonically to failure in four point bending using a hydraulic actuator. The longitudinal strain in the CFRP splice plate and the main plates was measured at several locations using electrical resistance strain gauges.

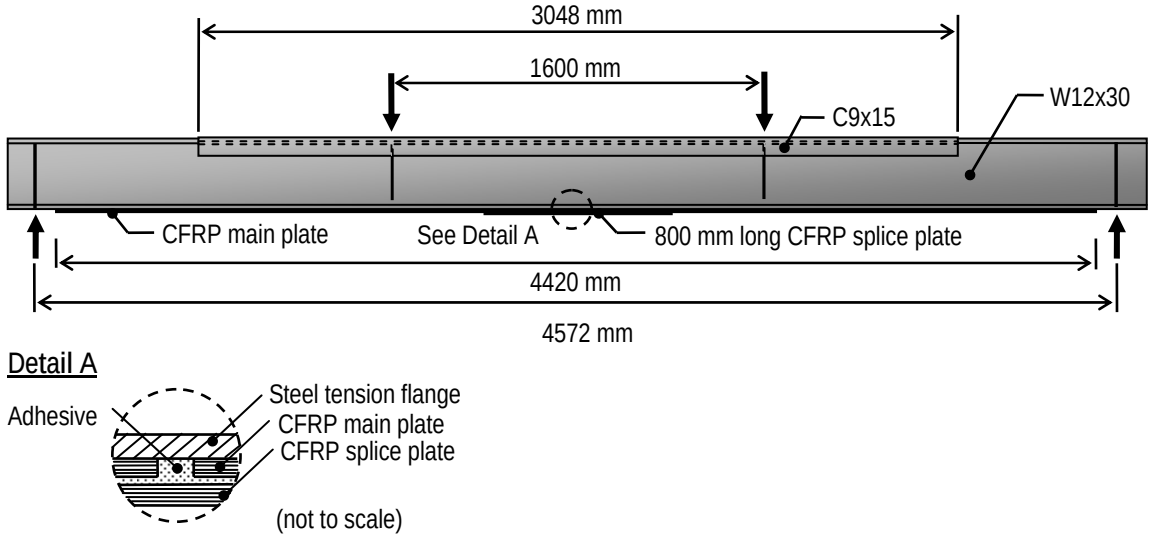

Figure 5 Typical steel test beam configuration

Experimental Results

Results of the Double-lap Shear coupon Tests

The measured load-strain behavior for all three of the joint configurations at the center of the splice joint is shown in Figure 6. The initial stiffness of all three joints was similar up to a load level of 40 kN. At the 40 kN load level a sudden increase of the measured strain was observed for joints A and B. This was likely due to cracking of the adhesive within the joint due to a stress concentration near the square plate end at the center of the joint. Cracking of the adhesive resulted in a corresponding loss of stiffness of the joint as shown in Figure 6 (a). The load strain behavior of Joint C did not exhibit a similar increase which suggests the reverse taper was effective in reducing the stress concentration near the plate end. Joint A failed suddenly due to debonding of the CFRP splice plates at a load level of 90 kN. Failure occurred primarily by separation of the adhesive from the CFRP laminates as shown in Figure 6 (b). Joint B exhibited additional cracking at a load level of 144 kN and ultimately failed by debonding of the splice plates at a load level of 160 kN. Joint C failed at a load level of 190 kN suddenly due to debonding of the splice plates and did not exhibit any cracking throughout the entire loading range. The experimental results demonstrate that the presence of the reverse taper and the adhesive fillet details can approximately double the capacity of a bonded splice joint.

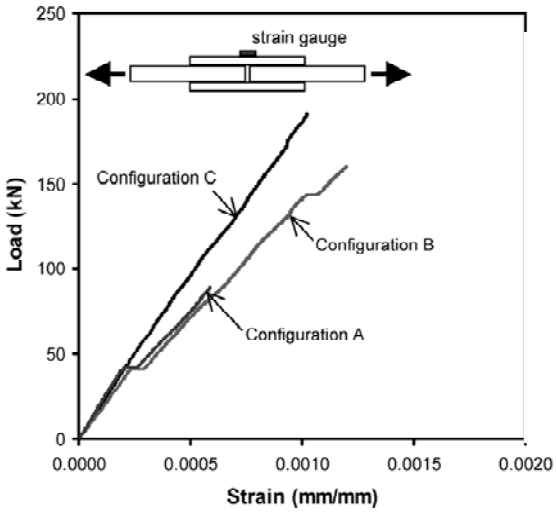

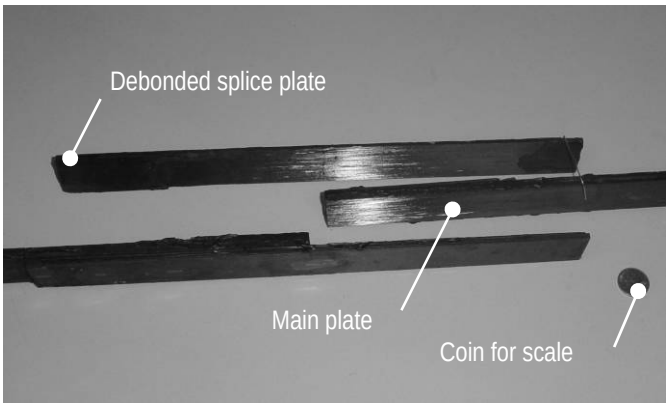

(a) Load-strain behavior (b) Typical debonding failure

Figure 6: Behavior of double-lap shear coupons

Based on the measured strains at various locations along the length of the splice plate, the corresponding longitudinal stress distribution was determined. The distribution of the measured longitudinal stress is presented in Figure 7(a) and (b) for joint configurations A and C respectively at a load level of 80 kN. An analytical model was previously developed by others to predict the distribution of longitudinal stress in the bonded cover plates of a double-lap shear coupon with square plate ends (Albat and Romilly, 1999). The calculated stress distribution using this model is also presented in Figure 7(a) and (b) for reference purposes. Inspection of Figure 7(a) indicates that the predicted stresses closely match the trend of the stresses measured for joint configuration A which was fabricated with square plate ends. Both the measured and the predicted stress distributions exhibit a sharp peak at the center of the joint. This verifies the presence of a significant shear stress concentration in the adhesive near this location. Inspection of Figure 7(b), however, indicates that the measured stress at the center of the splice joint for joint configuration C, which was fabricated with a reverse taper at this location, was significantly lower than that predicted by the analytical model. This further demonstrates that the reverse taper effectively helped to reduce the shear stress concentration which formed near the plate end.

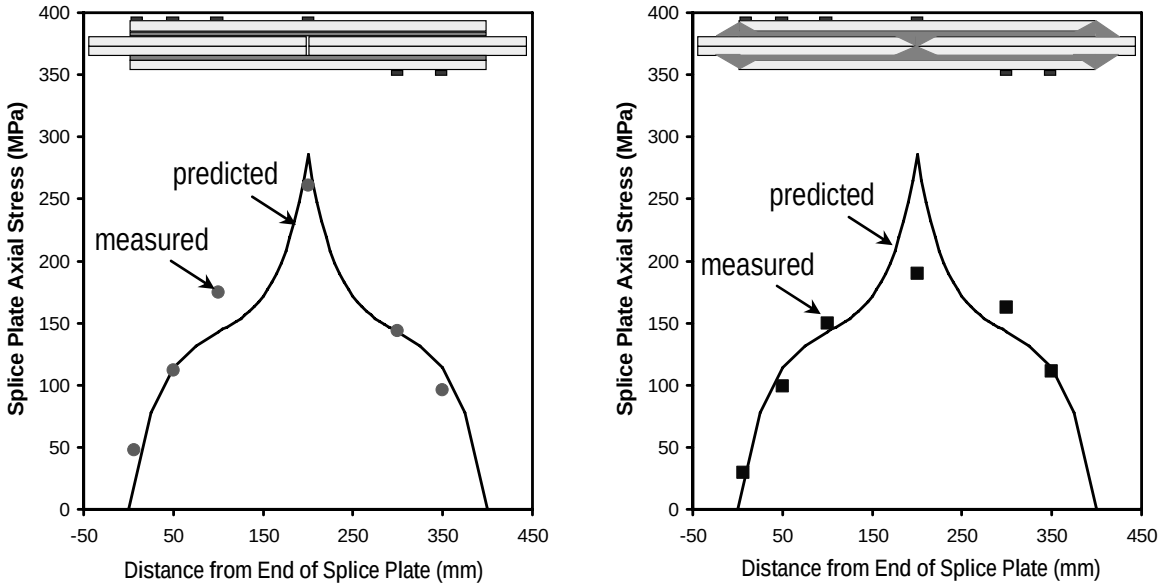

(a) Joint configuration A (b) Joint configuration C

Figure 7 Longitudinal stress distribution in the CFRP splice plate

Results of the Beam Tests

Both of the tested beams employed 800 mm long splice plates with square ends, similar to joint configuration A. Both beams failed due to debonding of the splice plates as shown in Figure 8. The total measured load immediately prior to debonding was 177 kN and 205 kN for each of the beams respectively. This corresponds to approximately 37 percent and 43 percent of the estimated yield load of the strengthened beams respectively as determined by a non-linear moment curvature analysis. Inspection of the first test beam after failure indicated that there were substantial air voids in the adhesive layer between the steel surface and the main CFRP plates which likely accounted for the slight variation of the failure load between the two beams.

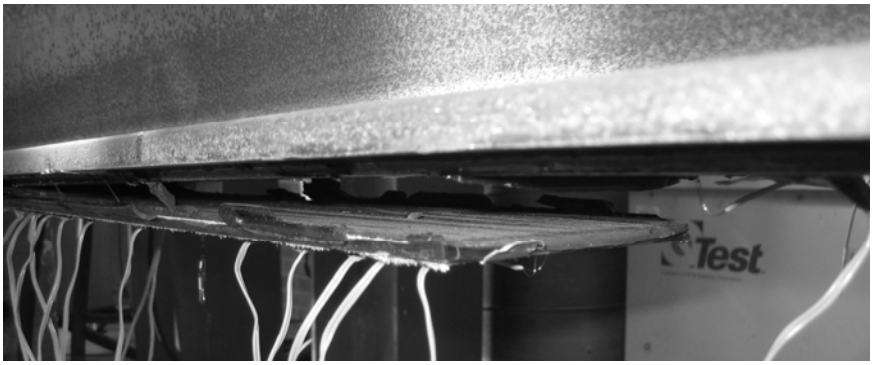

Figure 8 Typical debonding failure of the splice plate for the beam tests

The distribution of the longitudinal stress along the length of the splice plate, which was determined from the measured strains from the second beam test, is shown in Figure 9(a) for various load levels. The measured stress profile from the first test closely matched that shown in Figure 9 and therefore is not presented in this paper. Assuming that the stress in the splice plate is constant throughout the thickness of the plate, the average shear stress along a given interval of the adhesive layer can be determined from the longitudinal stresses at discrete locations as:

$$\bar{\tau} = \frac{\left(\sigma_i - \sigma_{i-1}\right)}{\left(x_i - x_{i-1}\right)} t_{FRP} \qquad \text{Equation (1)}$$

where $\bar{\tau}$ is the average shear stress along the interval under consideration, σ_i and σ_{i-1} are the longitudinal stresses in the splice plate at the i^{th} and the $(i-1)^{th}$ strain gauges respectively, and x_i and x_{i-1} are the locations of the i^{th} and the $(i-1)^{th}$ strain gauges respectively as measured from the end of the splice plate.

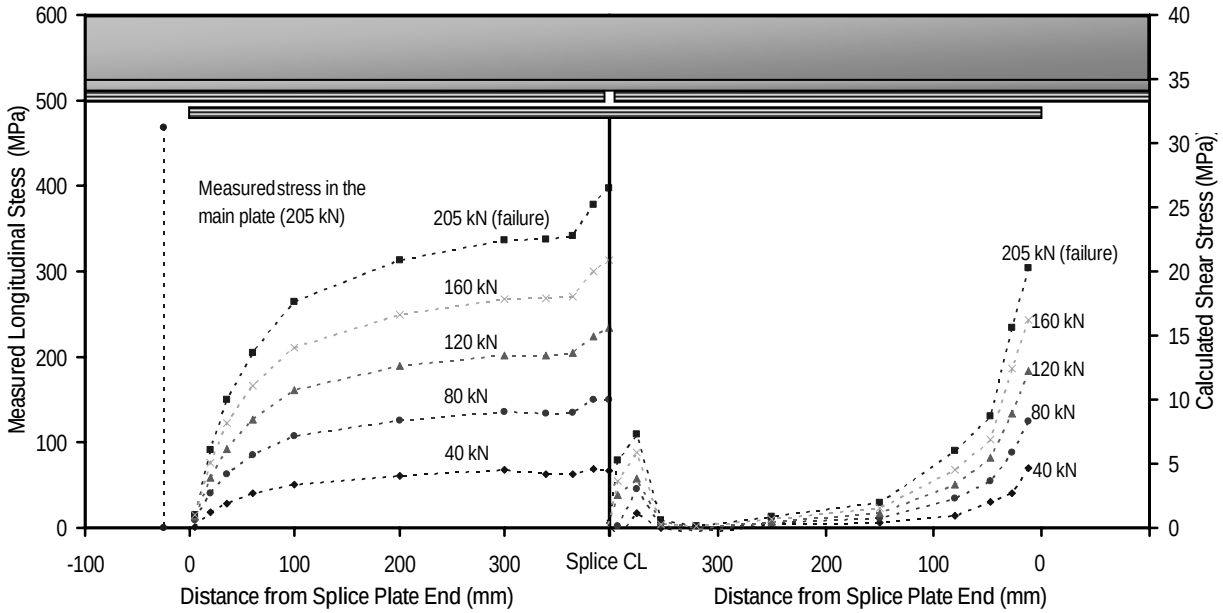

(a) Splice plate longitudinal stress (b) Adhesive shear stress

Figure 9 Typical longitudinal and shear stress distribution for the splice plates of the beam tests

The calculated bond shear stress distribution along the length of the splice plate is shown in Figure 9(b). Significant shear stress concentrations were calculated at localized regions near the end of the CFRP splice plate and near the center of the splice joint which can be observed in Figure 9(b). The maximum

calculated shear stress in the adhesive at a load level of 205 kN was 20 MPa near the end of the CFRP splice plate. At the same load level, the corresponding peak shear stress near the center of the splice was 7.3 MPa while the average calculated shear stress at a distance of 200 mm to 300 mm away from the splice plate end was only 0.9 MPa. This significant concentration of stresses near the plate ends is likely the cause of the premature debonding failure which was observed during both flexural tests. This highlights the need to investigate various details to help reduce the stress concentration near the plate ends.

Finite Element Analysis

A two-dimensional finite element model was also developed to predict the bond stress distributions along the length of an adhesively bonded joint. The model was used to predict the stress distributions for the square ended double-lap shear coupon which was tested as joint configuration A in the experimental program. The coupon was modeled using standard 8-node quadratic elements with an average side length of approximately 1 mm. A quarter of the coupon was modeled using the symmetry boundary conditions and a tensile load of 80 kN was applied along the longitudinal axis of the coupon. The adhesive was modeled as an isotropic material and the CFRP was modeled as an orthotropic material using the material properties given in Table 2.

Table 2 Material properties for Finite Element Analysis

	Adhesive*	**CFRP**
Longitudinal Modulus, E_x	2,977 MPa	455,000 MPa
Transverse Modulus, E_y	-	10,200 MPa
Through Thickness Modulus, E_z	-	10,200 MPa
Poison's Ratio, ν_{xy}	0.39	0.33
Poison's Ratio, ν_{yz}	-	0.33
Poison's Ratio, ν_{zx}	-	0.33
Shear Modulus, G_{xy}	-	3,750 MPa
Shear Modulus, G_{yz}	-	3,750 MPa
Shear Modulus, G_{zx}	-	3,750 MPa

*Only E and ν were defined for the adhesive

The deformed shape of the finite element mesh near the end of the CFRP splice plate is shown in Figure **10**(a). The effect of peeling at the plate end due to the localized bending effect is evident in the figure. This effect is due to the eccentricity of the CFRP splice plate relative to the applied load. A similar behavior was observed near the center of the splice joint. From the finite element analysis, the longitudinal stress distribution along the length of the splice plate was determined at three different levels through the thickness of the CFRP splice plate: at the top surface of the splice plate, at the mid-thickness of the plate and at the interface between the adhesive and the CFRP. The distribution of the longitudinal stresses at each of these three levels is shown in Figure 10(b). The longitudinal stress distribution as measured experimentally at the top surface of the CFRP splice plate for joint configuration A is also plotted in the figure for comparison purposes. Figure 10(b) indicates that the localized curvature of the splice plate near the ends of the CFRP plates has a noticeable effect on the distribution of the longitudinal stresses in the splice plate. Near the end of the splice, the curvature of the plate induces a longitudinal compressive stress at the top surface of the plate while inducing a slightly higher tension stress at the CFRP-adhesive interface. A similar trend is observed near the center of the splice plate as can be seen in Figure 10(b). The finite element results exhibit a similar trend and demonstrate a relatively good correlation with the measured strains in the splice plate.

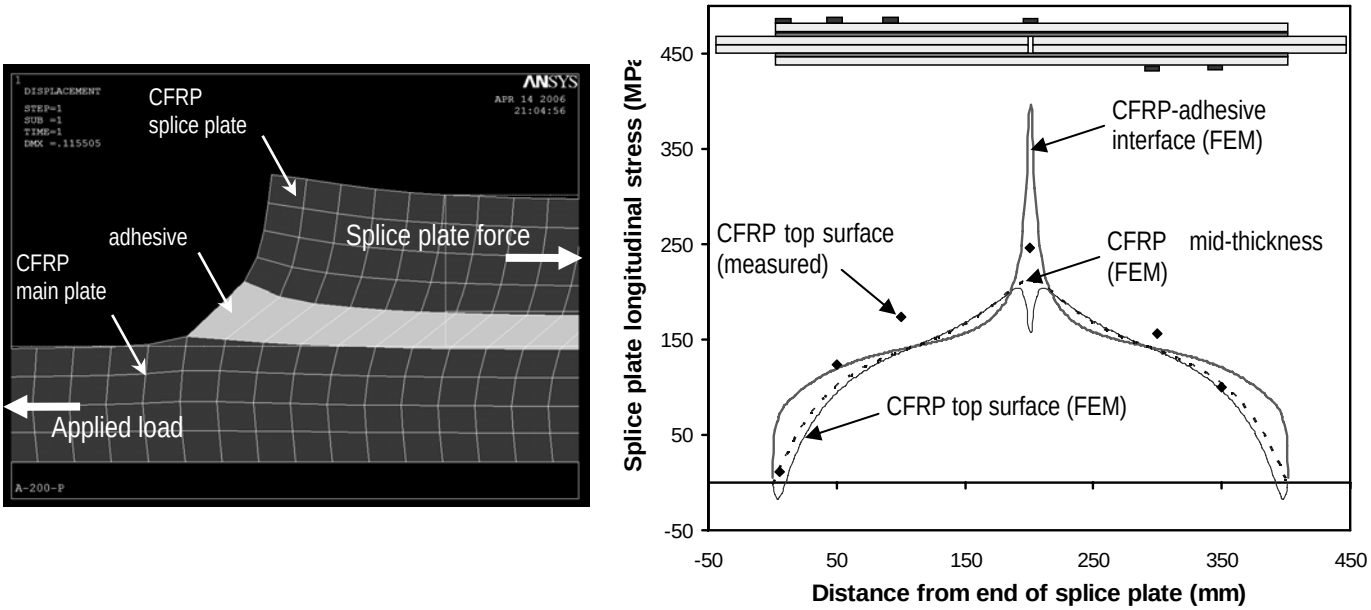

(a) Localized deformed shape (b) Longitudinal stress distribution

Figure 10 Finite element analysis results of joint configuration A (square plate ends)

CONCLUSIONS

This paper presents the findings of an extensive research program which was conducted to investigate the fundamental characteristics of the behavior of steel-concrete composite beams strengthened with high modulus CFRP materials. The findings indicate that high modulus CFRP materials can be used to increase the elastic stiffness, flexural yield strength and ultimate moment capacity of steel bridges and structures. The paper also proposes flexural design guidelines which can be used to design the required CFRP strengthening materials to achieve a desirable increase of the allowable live load capacity of a steel-concrete composite beam. Based on the findings of double-lap shear coupon tests, it is apparent that the implementation of a reverse-taper joint configuration can effectively increase the debonding strength of CFRP bonded joints and splices. Additionally, closed form analytical tools and finite element analysis techniques can be used to predict the bond behavior of CFRP bonded joints. The findings of this paper indicate that high modulus CFRP materials represent an effective method to strengthen and retrofit steel bridges and structures.

ACKNOWLEDGEMENTS

The authors would like to acknowledge the contributions of Mitsubishi Chemical FP America Inc. and the support provided by the National Science Foundation (NSF) Industry/University Cooperative Research Center (I/UCRC) for Repair of Buildings and Bridges with Composites (RB^2C).

REFERENCES

- Al-Saidy, A.H., Klaiber, F.W. & Wipf, T.J. (2004). Repair of steel composite beams with carbon fiber-reinforced polymer plates. *Journal of Composites for Construction, 8 (2),* 163-172.
- American Institute of Steel Construction. (2001). Manual of steel construction: load and resistance factor design. Third edition.
- Belingardi, G., Goglio, L. & Tarditi, A. (2002). Investigating the effect of spew and chamfer size on the stresses in metal/plastics adhesive joints. *International Journal of Adhesion and Adhesives, 22,* 273-282.
- Buyukozturk, O. Gunes, O. & Karaca, E. (2004). Progress in understanding debonding problems in reinforced concrete and steel members strengthened using FRP composites. Construction and Building Materials, 18, 9-19.
- Dawood, M. (2005). Fundamental Behavior of Steel-Concrete Composite Beams Strengthened with High Modulus Carbon Fiber Reinforced Polymer (CFRP) Materials. Master's Thesis, North Carolina State University, Raleigh, North Carolina.

- Hildebrand, M. (1994). Non-linear analysis and optimization of adhesively bonded single lap joints between fibre-reinforced plastics and metals. International Journal of Adhesives, 14 (4), 261-267.
- Lenwari, A., Thepchatri, t. & Albrecht, P. (2005). Flexural response of steel beams strengthened with partial-length CFRP plates. *Journal of Composites for Construction, July/August*, 296-303
- Lenwari, A., Thepchatri, T. & Albrecht, P. (2006). Debonding strength of steel beams strengthened with CFRP plates. *Journal of Composites for Construction, January/February*, 69-78
- Liu, X., Silva, P. & Nanni, A. (2001). Rehabilitation of steel bridge members with FRP composite materials. In Figueiras, J., Juvandes, L. & Furia, R. (Eds.), Proceedings of CCC 2001, composites in construction (pp. 613-617).
- Mertz, D.R. & Gillespie Jr., J. W. (1996). Rehabilitation of steel bridge girders through the application of advanced composite materials (Contract NCHRP-93-ID011). Washington, D.C.: Transportation Research Board.
- Miller, T.C., Chajes, M.J., Mertz, D.R. & Hastings, J.N. (2001). Strengthening of a steel bridge girder using CFRP plates. *Journal of Bridge Engineering, 6 (6)*, 514-522.
- Rizkalla, S. and Dawood, M. (2006). High modulus carbon fiber materials for retrofit of steel structures and bridges. Accepted for publication in the proceedings of *ACUN-5 International Composites Conference "Developments in Composites : Advanced, Infrastructural, Natural and Nano-composites*". July 11-14, 2006. Sydney, Australia.
- Schnerch, D. (2005). Strengthening of steel structures with high modulus carbon fiber reinforced polymer (CFRP) Materials. Ph.D. dissertation, North Carolina State University, Raleigh, North Carolina.
- Schnerch, D., Dawood, M., Rizkalla, S. and Sumner, E. (2006). Proposed design guidelines for strengthening of steel bridges with FRP materials. Construction and Building Materials, accepted for publication
- Sen, R., Libby, L. & Mullins, G. (2001). Strengthening steel bridge sections using CFRP laminates. *Composites Part B: Engineering, 39*, 309-322.
- Smith, S.T. & Teng, J.G. (2001). Interfacial stresses in plated beams. Engineering Structures, 23, 857-871.
- Stallings, J.M. and Porter, N.M. (2003). Experimental investigation of lap splices in externally bonded carbon fiber-reinforced plastic plates. *ACI Structural Journal, 100 (1)*, 3-10.
- Stratford, T. & Cadei, J. Elastic analysis of adhesion stresses for teh design of a strengthening plate bonded to a beam. *Construction and Building Materials, 20*, 34-45.
- Tavakkolizadeh, M. & Saadatmanesh, H. (2003). Strengthening of steel-concrete composite girders using carbon fiber reinforced polymer sheets. *Journal of Structural Engineering, 129 (1)*, 30-40.